Numerical Analysis of the Changes in Dense Medium Feed Solids on Dense Medium Cyclone Performance

M. Narasimha [1*] **, M. S. Brennan** [1] **, P.N. Holtham** [1] **and P. K. Banerjee** [2]

[1] Julius Kruttschnitt Mineral Research Centre,
The University of Queensland, Isles Road, Indooroopilly 4068, Queensland, Australia.

[2] R&D Division, Tata Steel, Jamshedpur, Jharkhand 831 007, India.

Abstract

Numerical simulations of changes in feed medium solids on dense medium cyclone performance were performed using a multi-phase mixture CFD (Computational Fluid Dynamics) model for medium and air-core coupled with Lagrangian model for coal particles for a 350mm DSM cyclone. The turbulence was resolved using Large Eddy Simulation (LES). The mixture model considered the interactions between water and solid phases in terms of hindered settling, lift and Bagnold forces at high feed medium solid loadings. The medium properties were modified by changing the particle size distribution and concentration. Three different medium sizes (ultrafine, superfine and fine) were used in the simulations. The effect of medium stability and rheology on DMC performance is related to feed medium size in terms of density differential and medium segregation. The simulations predicted low Ep (Ecort probability) values with finer medium which gives high separation efficiency on density. A reduction in cyclone efficiency observed for a given feed medium solids distribution at higher feed medium concentrations due to an increase in slurry viscosity.

Introduction

Medium behaviour plays an important role in dense medium cyclone (DMC) separation. Remarkable advances have been made in the knowledge of the properties of dense suspensions and of their influence on separation sharpness. This has led to improved operation of DMCs [1-4]. Medium properties that are related to medium rheology and stability will be controlling the separation of coal particles in DMCs. The factors that control the medium properties are particle size distribution, particle shape, density (solid content) and medium contamination. The influences of these factors on DMC performance have been addressed by various researchers. However, conflicting conclusion have often been drawn.

The effect of magnetite particle size was studied by Fourie et al [5] and Chedgy et al [6] who observed that by using progressively finer magnetite the separation efficiency was improved, due to the increase in medium stability. An opposite trend was observed by Stoessner [7] while studying the effect of finer magnetite on DMCs. He observed that the fine magnetite does not perform as well as coarse commercial magnetite. He attributed this to the deleterious effect of viscosity on DMC performance. A similar effect was also reported by Collins et al [8] when working at high medium densities in iron ore separation. Davis and Napier-Munn [9], in studying the effect of medium contamination on cyclone performance, showed that the clay contamination significantly reduced the separation efficiency due to an increased effect of medium viscosity. Later He and Laskowski [3] studied the medium stability and rheology

on DMC performance in a 6 inch DSM body and observed that while the separation efficiency and cut point shift for coarse particles (>2 mm) were mainly determined by the medium stability, the separation performance of fine particles (<0.5 mm) was more sensitive to the change in medium rheology.

Although the medium rheology is determined by the medium composition, researchers more often interpret the effect of medium properties on DMC performance in terms of the medium composition. Collins [10] and Morimoto [11] found that the effect of medium density on separation efficiency was insignificant within a limited density range. In contrast, a reduction in cyclone efficiency at high feed medium densities was observed in detailed studies by He and Laskowski [3], Napier-Munn [12] and Wood [13]. This effect was attributed to increased viscosity and increased medium segregation near the apex zone.

DMC separation efficiency is also affected by medium stability. The appearance of density gradients due to flow reversals and turbulence fluctuations in the cyclone leads to the misplacement of feed particles, hence the reduction of separation efficiency. Davis [14] and Wood [13] in plant and pilot scale DMC tests noted that a higher density differential led to a longer retention time of near-density materials. The cyclone became unstable and periodically overloaded, resulting in a breakdown of the stable flow pattern and surging. Collins et al [15] recommended that for a stable separation the density differential be maintained within 0.2 and 0.5 s.g.

Understanding the effect of medium properties on DMC performance is complicated due to their dynamic nature, which can be attributed to complex non-Newtonian medium flow behaviour and the dominance of turbulence fluctuations. Although efforts have been made in the past to understand such relationships, medium rheology inside the cyclone has been rarely addressed. Experimental medium segregation studies inside a cyclone are very limited [16-18] and provide limited understanding of the medium rheology inside the cyclones.

Recently, CFD studies in dense medium cyclones have been successful in quantifying the medium segregation [19-22]. The CFD models provide plausible medium flow information with the right choice of multi-phase models. The predicted medium flow information can then be used to relate the performance of a DMC to the medium rheology inside the cyclone. Another key problem is the choice of turbulence model. The turbulence is too anisotropic to treat with a k-ε model and this has led some researchers to use the differential Reynolds stress turbulence model. However some recent studies [23-25] have shown that the LES technique gives better predictions of the velocities in cyclones and seems to do so on computationally practical grids.

In this paper, a CFD analysis of the effect of changes in the feed size distribution and the feed concentration of medium on the performance of 350 mm DSM pattern DMC are reported.
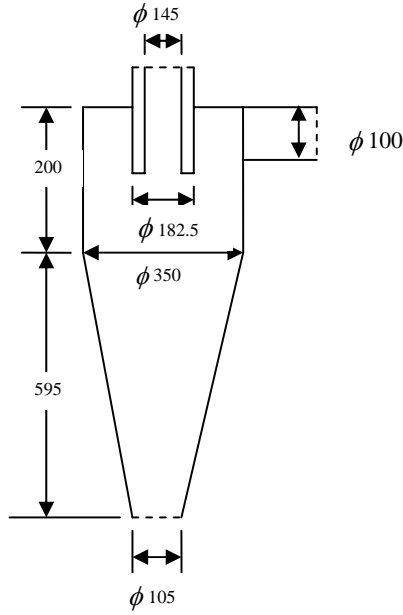
(a)
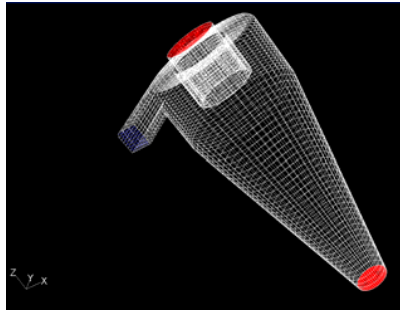
(b)

Fig 1: (a) Dimensions of the 350 mm DSM dense medium cyclone used for simulations, (b) Grid generated in Gambit.

MODEL DESCRIPTION

Turbulence Models

The basic CFD approach was the same as that used by Narasimha et al [21]. The simulations used Fluent with 3D body fitted grids and an accurate geometric model of the 350mm DSM pattern dense medium cyclone used by Subramanian [18] in his GRT studies. The dimensions of the cyclone are shown in Figure 1a and a view of the grid used in the simulations is shown in Figure 1b. The equations of motion were solved using the unsteady solver and represent a variable density slurry mixture:

$$\frac{\partial \rho_m}{\partial t} + \frac{\partial \rho_m u_{mi}}{\partial x_i} = 0 \tag{1}$$

$$\frac{\partial}{\partial t}(\rho_m u_{mi}) + \frac{\partial}{\partial x_j}(\rho_m u_{mi} u_{mj}) =$$
$$-\frac{\partial}{\partial x_i} p + \frac{\partial}{\partial x_j}(\tau_{\mu,ij} + \tau_{d,ij} + \tau_{t,ij}) + \rho_m g_i \tag{2}$$

The simulation are started as two phase simulations with just water and an air and these two phase simulations were used as an initial condition for the simulations with medium in the feed.

The flow in DMC is turbulent and the turbulence was treated with two different techniques. The Launder et al (1975) differential Reynolds stress turbulence model with the quadratic pressure strain correlation and Large Eddy simulation (LES) were used in the two phase simulations. The simulations with medium in the feed used LES with the standard Smagorinsky (1966) SGS model. In the DRSM simulations $\tau_{t,ij}$ in equation (2) denotes the Reynolds stresses , whilst in the LES simulations $\tau_{t,ij}$ denotes the sub grid scale stresses. $\tau_{d,ij}$ is the drift tensor and arises in equation (2) as part of the derivation of the Mixture model (Manninenn et al 1996). The drift tensor accounts for the transport of momentum as the result of segregation of the dispersed phases and is an exact term:

$$\tau_{d,ij} = \sum_{p=1}^{n} \alpha_p \rho_p u_{pm,i} u_{pm,j} \tag{3}$$

All equations were discretized using the QUICK option except that Bounded central differencing was used for momentum with the LES. PRESTO was used for Pressure and SIMPLE was used for the pressure velocity coupling. The equations were solved using the unsteady solver with a time step which was typically 5.0×10^{-4}s for both the DRSM simulations and LES simulations. The LES used the Spectral Synthesiser option to approximate the feed turbulence.

Multiphase modeling – mixture model with lift forces

The medium was treated using the Mixture model [27], which solves the equations of motion for the slurry mixture and solves transport equations for the volume fraction for any additional phases p, which are assumed to be dispersed throughout a continuous fluid (water) phase c:

$$\frac{\partial}{\partial t} \alpha_p + \frac{\partial}{\partial x_i}(\alpha_p u_i) + \frac{\partial}{\partial x_i}(\alpha_p u_{pm,i}) = 0$$
$$u_{pm,i} = u_{pi} - u_i \tag{4}$$

$u_{pm,i}$ is the drift velocity of phase p relative to the mixture m. This is related to the slip velocity $u_{pc,i}$, which is the velocity of phase *p* relative to the continuous water phase *c* by the formulation:

$$u_{pmi} = u_{pci} - \sum_{l=1}^{n} \frac{\alpha_k \rho_k}{\rho_m} u_{lci}$$
$$u_{pci} = u_{pi} - u_{ci} \tag{5}$$

Phase segregation is accounted for by the slip velocity which in Manninen et al's [27] treatise is calculated algebraically by an equilibrium force balance and is implemented in Fluent in a simplified form. In this work Fluent has been used with the granular options and the Fluent formulation for the slip velocity has been modified where (i) a shear dependent lift force based on Saffman's [28] expression and (ii) the gradient of granular pressure (as calculated by the granular options) have been added as additional forces. Adding the gradient of granular pressure as an additional force effectively models Bagnold dispersive forces [29] and is an enhancement over our earlier work [21].

$$u_{pci} = \frac{d^2{}_p(\rho_p - \rho_m)}{18 f_{rep}\mu_c} *$$

$$\begin{pmatrix} g_i - \dfrac{\partial}{\partial t}u_{mi} - u_{mj}\dfrac{\partial}{\partial x_j}u_{mi} + \\[2mm] 0.75\dfrac{\rho_c}{\rho_p - \rho_m}C_{lp}\varepsilon_{ijk}\omega_{mj}u_{pck} - \dfrac{1}{\alpha_p(\rho_p - \rho_m)}\dfrac{\partial}{\partial x_i}P_{pg} \end{pmatrix} \quad (6)$$

Equation (6) has been implemented in Fluent as a custom slip velocity calculation using a user defined function, f_{rep} has been modelled with the Schiller Naumann drag law [30] but with an additional correction for hindered settling based on the Richardson and Zaki [31] correlation:

$$f_{rep} = (1 + 0.15\,\mathrm{Re}_p{}^{0.687})\alpha_p{}^{-4.65} \quad (7)$$

The lift coefficient has been calculated as

$$C_{lp} = 4.1126\left(\frac{\rho_f d_p{}^2|\omega|}{\mu_c}\right)f_c \quad (8)$$

f_c corrects the lift coefficient using the correlation proposed by Mei [32].

Medium rheology

The mixture viscosity in the region of the cyclone occupied by water and medium has been calculated using the granular options where the Gidaspow granular viscosity model [33] was used. The Gidaspow model [33] makes the viscosity as shear dependant.

Medium with size distribution

The mixture model was set up with 8 phase transport equations, where 7 of the equations were for medium which was magnetite with a particle density of 4950 kg.m-3 and 7 particle sizes which were; 2.4, 7.4, 15.4, 23.8, 32.2, 54.1 and 82.2 μm. The seventh phase was air, however the slip velocity calculation was disabled for the air phase thus effectively treating the air with the VOF model [35]. The volume fraction of each modeled size of medium in the feed boundary condition was set so that the cumulative size distribution matched the cumulative size distribution of the medium used by Subramanian [18] and the total feed medium concentration matched Subramanian's experimental feed medium concentrations.

Coal particle tracking model

In principle, the mixture model can be used to model the coal particles as well as medium but the computational resources available for this work limited simulations using the mixture model to around 9 phases, and it was impractical to model coal with more than two sizes or densities simultaneously with 6 medium sizes. Thus the Fluent discrete particle model (DPM) was used where particles of a known size and density were introduced at the feed port using a surface injection and the particle trajectory was integrated through the flow field of a multiphase simulation using medium. This approach is the same as that used by Suasnabar [19].

Fluent's DPM model calculates the trajectory of each coal particle d by integrating the force balance on the particle, which is given by equation (9):

$$\frac{Du_{d,i}}{dt} = k_d(u_{m,i} - u_{d,i}) + g_i\left(\frac{\rho_d - \rho_m}{\rho_d}\right) \quad (9)$$

k_d is the fluid particle exchange coefficient:

$$k_d = \left(\frac{18\mu_m d_d^2}{\rho_d}\right)\left(\frac{C_D\,\mathrm{Re}_d}{24}\right) \quad (10)$$

The presence of medium and the effects of medium segregation are incorporated in the DPM simulations because the DPM drag calculation employs the local mixture density and local mixture viscosity which are both functions of the local medium concentration. This intrinsically assumes that the influence of the medium on coal partitioning is a primarily continuum effect. i.e., the coal particles encounter (or "see") only a dense, high viscosity liquid during their trajectory. Further the DPM simulations intrinsically assume that the coal particles only encounter the mixture and not other coal particles and thus assume low coal particle loadings.

To minimize computation time the DPM simulations used the flow field predicted by the LES at a particular time. This is somewhat unrealistic and assumes one way coupling between the coal particles and the mixture.

RESULTS AND DISCUSSIONS

Velocity Predictions

The predicted two phase velocity field inside the DSM geometry is similar to velocities predicted in hydrocyclones using LDA. There was no measured flow field data available in 350 mm DSM body, but does exist for a 100 mm cyclone of the same shape. The velocities predicted by the CFD were compared on the 100 mm cyclone using RSM (Reynolds turbulence model) and LES turbulence models. An optimum grid size of 110, 000 is used on 100 mm cyclone for two phase flow simulations. Predicted flow velocities in a 100mm DSM body were compared with experimental LDA data [36] and shown in Fig 2(a) and 2(b). Predicted velocity profiles are in agreement with the experimental data of Fanglu and Wenzhen [36], measured by laser doppler anemometry.

(a)

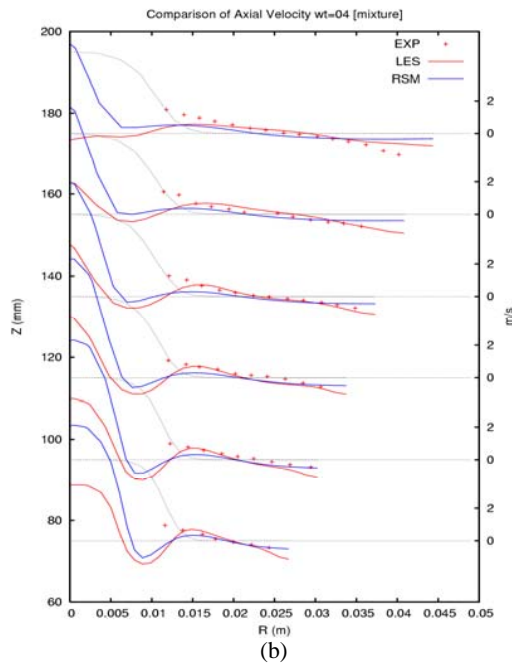Comparison of Axial Velocity wt=04 [mixture]
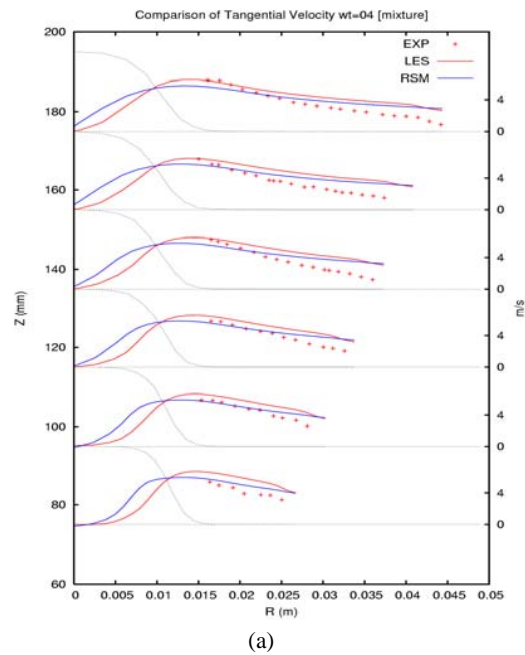
Fig.2. Comparison of predicted (a) tangential velocity field, (b) axial velocity field with experimental data (Fanglu and Wenzhen (1987)).

Rheology of the medium

Three different medium sizes (ultrafine, superfine and fine) were used in the simulations. The size distributions are described in Table 1. The rheological flow curve for superfine magnetite has been discussed in the following section.

Table 1: Particle size distribution of the tested magnetite samples

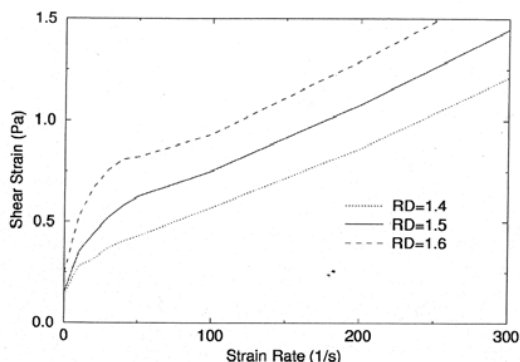| Magnetite sample	$d_{63.2}(\mu m)$	(Rosin-Rammler-Bennett constant) m
Fine	30.5	3.2
Superfine	20	1.6
ultrafine	17	1.45

Fig 3: Rheological flow curve for superfine magnetite at different feed densities [3]

Figure 3 shows the rheological curves for the tested super fine magnetite suspension for magnetite volumetric contents from 11% to 25% (the magnetite medium density range of 1.4 to 1.6). As Figure 3 demonstrates, the flow curves exhibit shear-thinning properties with yield stress. The differences between the yield

stress values are obviously very different for various grades of magnetites [3]. These flow curves could be fitted well with the Casson viscosity model. Further, the figure illustrates the effect of solid (magnetite) content for the superfine magnetite sample on the shear rate and yield stress. At high shear rates, the medium behaves like a Newtonian fluid. Eventually, the apparent viscosity of slurry medium will be calculated using by fitting Casson viscosity model eq (11) on shear stress vs shear rate data.

$$\tau = \left[\tau_c^{1/2} + (\eta_c D)^{1/2} \right]^2 \tag{11}$$

In DMCs, the magnetite medium particles are subjected to the centrifugal forces. This effect results in differences in densities between cyclone overflow and underflow which characterize the medium stability under dynamic conditions.

Comparison of predicted density profile with GRT experimental data:

Figure 4 shows the density profiles predicted by the CFD at steady flow for a feed RD of 1.465 and a feed head of 9Dc (equivalent to a volumetric flow rate of 0.0105 m^3 s^{-1}) together with an experimentally measured density profile for the same feed conditions from Subramanian [18]. Figure 3a shows the density profile for the CFD work and Figure 3b shows the gamma ray tomography density profiles. It is observed that the predicted density profiles are in good agreement with the experimental data and the complete validation was published elsewhere [21].

Further it is evident from Figure 4 that there is a narrow region close to the air core where the density of the medium is lower than the feed medium density. The particles that were centrifuged displaced the water towards the air core and this resulted in water being preferentially discharged via the overflow along with the particles in the lower size fractions, thus lowering the overflow density in comparison to that of the feed. The remaining medium has a density higher than that of the feed as the coarse size solid particles mostly affected by the centrifugal forces. The prevalence of a higher density of the medium within the cyclone also suggests that the residence time of water is lower than that of the solids.
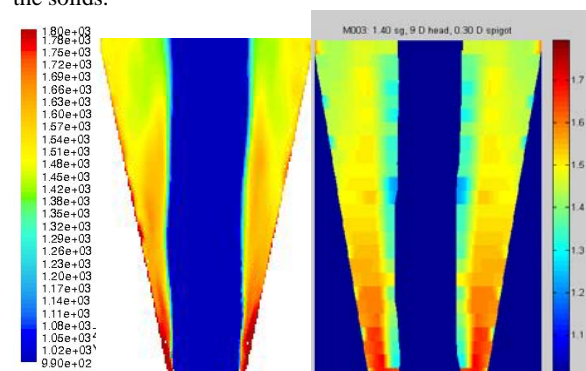
(a) CFD model   (b) Experimental – Subramanian (2002)

Figure 4: Comparison between predicted slurry densities (a) LES-Mixture latest work (see text left) (b) Experimental - Subramanian, 2002 for feed RD of 1.465, Feed head = 9D$_c$ (Q$_f$ = 0.0105 $m^{-3}s^{-1}$); in elevation.

Shear rate in DMC:

The shear rate within a dense medium cyclone is calculated using the predicted velocity gradients. The shear rate in DMC is

proportional to the angular velocity of the medium circulating inside the cyclone except near the air-medium interface. As shown in Fig 5(a) and (b), maximum shear rate within medium occurs at the point of maximum tangential velocity adjacent to the air core, resulting in a shear rate of 25 to 100 s^{-1} within the cylindrical and upper conical section of the cyclone. In entire cyclone, the maximum shear rate occurs near the air core/medium interface and apex zone.
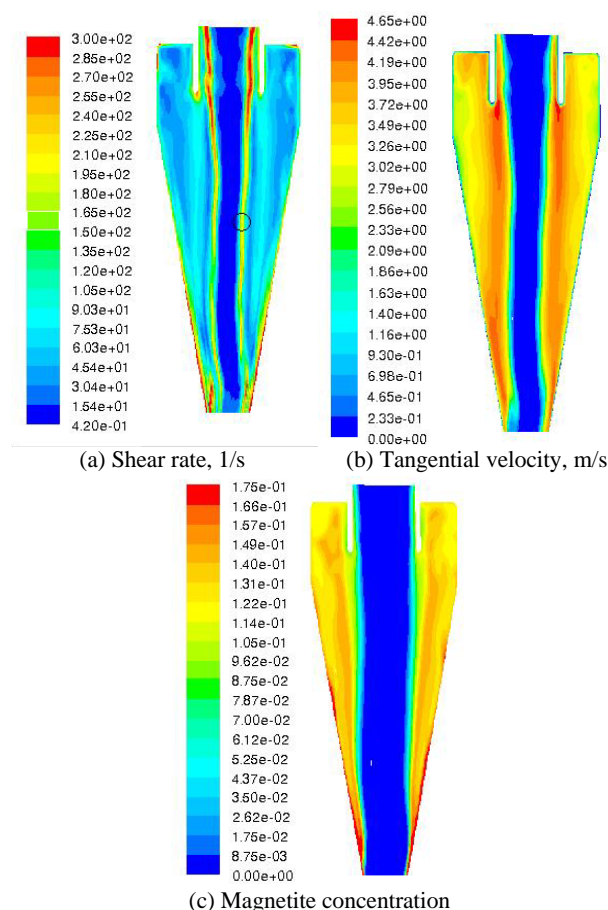

(a) Shear rate, 1/s   (b) Tangential velocity, m/s

(c) Magnetite concentration

Fig 5: Contour plots of (a) shear rate, (b) Tangential velocity, (c) magnetite concentration in DMC for superfine magnetite.

The high shear rates (~300 s^{-1}) resulting from large velocity gradients (see Figure 5(b)) persisted near the air core and large velocity and magnetite concentration gradients near the apex region are shown in Figure 5(c). Excluding the air core region, it is observed that the medium shear rate increases axially from top to bottom of the cyclone. These high shear rates are responsible for the presence of high viscosity region near the apex zone (see Figure 6).

Viscosity of the medium in DMCs:

From Figure (6) and (7), and also referring Figure 2, the viscosity of medium changes from an apparent viscosity of 3cp at the cyclone wall to 1cp adjacent to the air core. Apart from the wall, the viscosity of medium is high in the middle of the cyclone due the segregation of magnetite solids in this region. This indicates that medium near the air core would have less solids and, therefore, the viscosity at the air core would be lower, and the viscosity at the cyclone wall would be higher. Near the apex zone (see Fig 7), as indicated by circle, due to accumulation of the magnetite solids (as shown in Figure 5(c)) the viscosity is very high compare to all other cyclone regions.
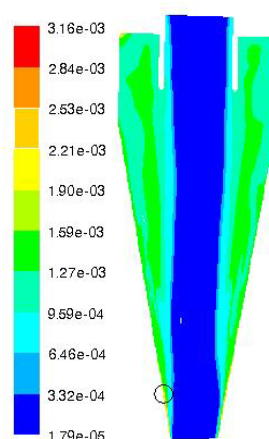

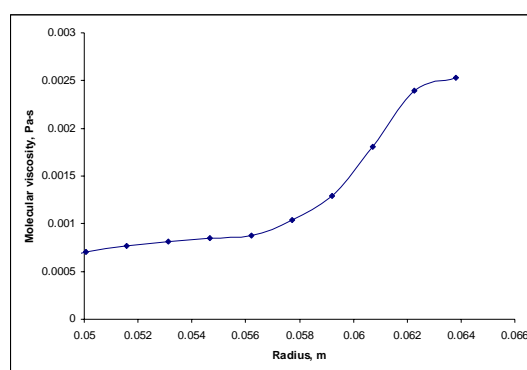Fig 6: Medium viscosity inside DMC for superfine magnetite

Figure 7: Radial variation of viscosity of medium at apex zone.

Stability of the dense medium in DMCs:

Stability of the magnetite is important factor in determining the performance of a dense medium cyclone. Stability is defined as the degree of stratification of particles within the fluid. The overall stability is provided by particle interaction, due to both direct inter-particle contact and the net influence of the forces of attraction and repulsion of the magnetite. Therefore, the stability of the medium is a measure of the homogeneity of these particles in the suspension.

In general, instability in a DMC is indicated by a high relative density differential between the underflow and overflow of the cyclone. This is caused by the medium particles centrifuging to the outer wall of the cyclone, thus increasing the relative density in this region. This may result in frequent surging in DMCs while separating coal.

Using the CFD model for the given magnetite size distributions, the density differentials between underflow and overflow were calculated and tabulated in Table 2. From Table 2, it is observed that medium stability higher for ultrafine magnetite than other two mediums, as indicated by low density differential between underflow and overflow.

Table 2: Predicted density differential for a feed RD@1.465, at feed head = 9 Dc,

Magnetite	rho_u	rho_o	diff
Fine	2218	1267	951
Superfine	1987	1339	648
ultrafine	1949	1326	623

Effect of feed size distribution on medium segregation:

The medium properties were modified by changing the particle size distribution. Three different medium sizes (ultrafine, superfine and fine) were used in the simulations and comparisons of medium segregation are shown in Figure 8. From Figure 6a and 8b, it is observed that segregation of medium is very significant in case of fine magnetite compared to ultrafine and superfine quality. As the fine magnetite has a predominantly coarser size distribution compared to ultrafine magnetite, the segregation or classification of these coarse particles at wall eventually builds high medium density near the underflow as well at wall region. The small magnetite particles are also classified and segregate in a region close to the air core, and eventually report to overflow. This medium segregation results a very high density differential between underflow and overflow as shown in Table 2.
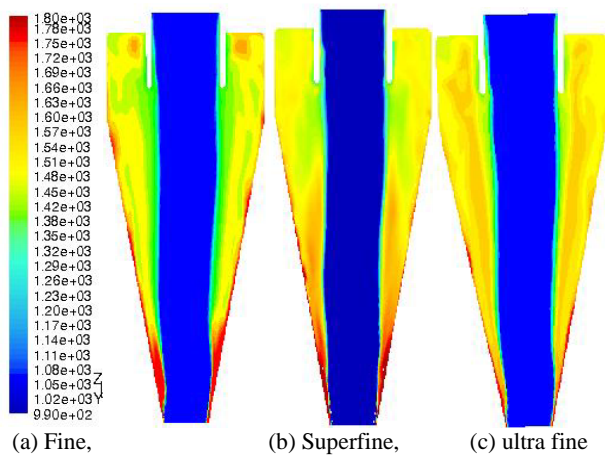
(a) Fine,　　　　　(b) Superfine,　　　(c) ultra fine

Fig 8: Contours of medium density for (a) fine, (b) superfine and (c) ultrafine quality in DMC

In the case of ultrafine medium flow simulation, the segregation of magnetite is less predominant than that of fine magnetite case. The magnetite concentration is almost all uniform across the radius from air core to the cyclone wall. The very fine particle fraction in the classified medium reports to overflow. This fine particles flow causes the appearance of slightly higher density in the middle of the cyclone (see the Fig 8c) compared to other regions. This result in to slightly higher overflow density and low density differential compare to the fine magnetite case.

In the case of superfine medium, which is having the predominant intermediate size fractions of magnetite particles, the medium segregation lies in between ultrafine and fine magnetite cases. As shown in Table 2, the density differential between underflow and overflow is some what higher than the ultrafine medium segregation and lower than the fine medium segregation.

Effect of feed solids concentration on medium segregation:

Medium segregation was studied with superfine magnetite at three feed solids concentrations (6.12, 7.5 and 11.62 % by volume), corresponding to medium densities of 1245, 1300 and 1465 kg m^{-3}. Comparison of density contours between the measured densities of Subramanian [18] and the medium densities predicted using the CFD model are shown in Figure 9 and are in good agreement. The quantitative density comparisons are made elsewhere [22].

(a) RD@1.245 GRT data (left side) and CFD data (right side)

(b) RD@1.3 GRT data (left side) and CFD data (right side)

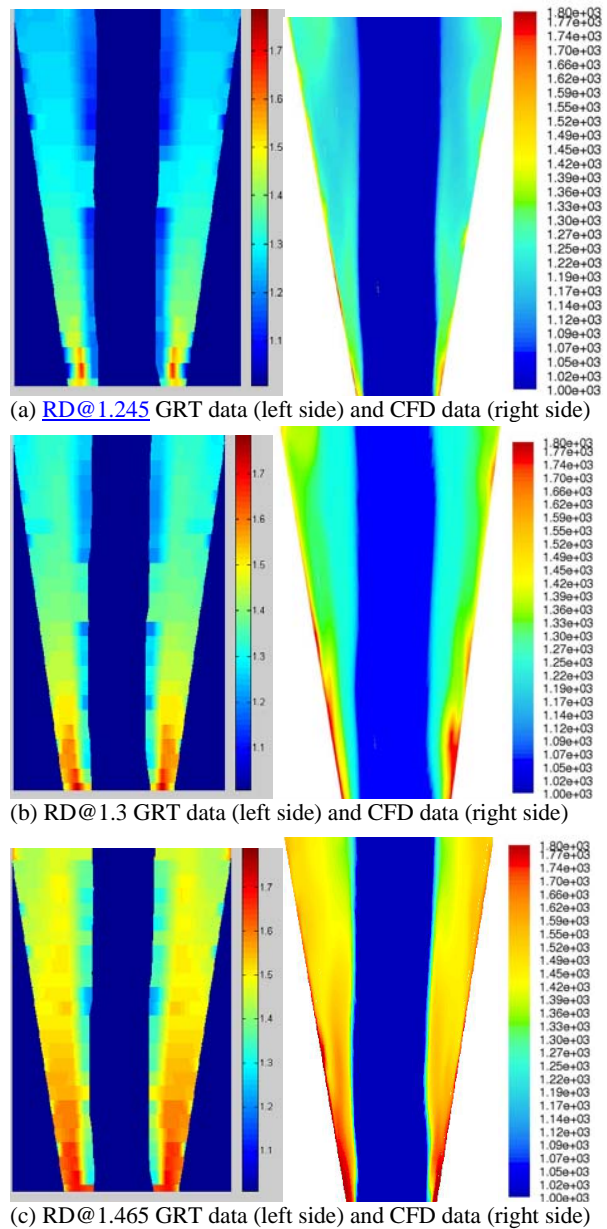(c) RD@1.465 GRT data (left side) and CFD data (right side)

Fig 9: Comparison between measured medium density contours (left side) by Subramanian (2002) and predicted medium density contours (right side) by CFD model at different feed medium relative densities (a) RD@1.245, (b) RD@1.3, and (c) RD@1.465 respectively.

From Figure 9, it is observed that an increase in the medium density increases the density gradient across the radius of cyclone from the air core to the wall of the cyclone. Also the axial medium segregation increases; hence an increase in density differential is expected (see the fig 10). This effect can be interrelated with changes of medium viscosity in the DMC [3 & 12]. It is expected that an increase in the feed solids concentration increases the medium viscosity. This increase in slurry viscosity at higher feed medium densities increases the drag on solid particles, which has the effect of reducing the particle terminal velocity, giving the particles less time to settle. This results an increased flow resistance of solid particles and further accumulation of solids near the wall and also at the bottom of the cyclone.
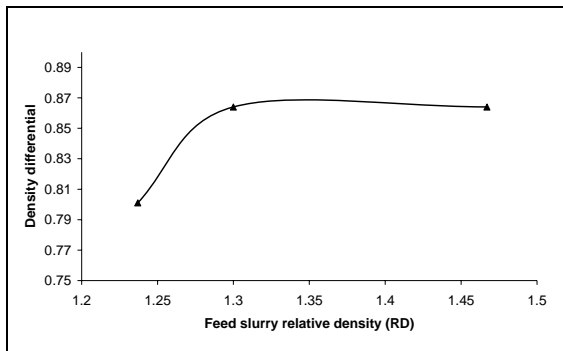
1047

Fig 10: Predicted density differential at various feed relative densities for superfine magnetite in DSM body

Effect of feed solids distribution and concentration on the performance of DMC:

The flow of coal particles in a DSM cyclone was modelled using discrete particle model (DPM) available in the FLUENT software. Pure coal particles in the range of 12000 to 1800 kg m^{-3} with different size (=8mm to 0.5mm) used for the studies. Before coal particle tracking, simulations were run with slurry (water and magnetite size distribution), to determine the velocity distribution of medium inside the cyclone. Then, coal particles of uniform size were injected through the inlet surface of the separator and their flow paths within the cyclone were tracked. The outlet stream in which the each particle reported was noted and the separation characteristics of the cyclone were determined. Each run was repeated five times and the average value was noted. During each run, 1050 particles of same size were injected simultaneously. Simulation runs were repeated for coal particles of different size. These data were then used to generate the partition curve of the DSM cyclone and to predict the cut density. The sharpness of cut of a dense medium cyclone is characterised by E_p, which is calculated by the following formula:

$$E_p = \frac{\rho_{75} - \rho_{25}}{2}$$

where ρ_{75} and ρ_{25} are the densities on the partition curve at 75% and 25% reject respectively. A small E_p implies a sharper cut and therefore better performance.

The effect of the feed medium concentration on the intrinsic separating ability of DMC is shown in Figure 11 for typical operating conditions. As seen from Figure 11, the increased feed medium density resulted in a general increase in Ep values. Hence lower efficiency at higher feed medium densities is expected. This efficiency drop can be correlated with the density differentials observed at higher feed medium densities. The density differential between cyclone underflow and overflow characterizes the medium stability as explained earlier. For typical operating conditions in coal preparation plants, the density differential is mostly affected by medium properties [3]. More fundamentally, at high medium densities (high concentrations), solid particles will have short response time and tend to misplacement to wrong products. The instability of dense medium separation is predominately high at high feed medium densities due to high density differentials.

It is observed that segregation of medium is very significant with variation of the quality of magnetite that used in DMC operation. The experimental studies on the effect of the medium size distribution on DMC (He and Laskowski (1994)) revealed that the separation performance of coarse coal particles (>2 mm) were strongly influenced by the medium stability not by the medium rheology.
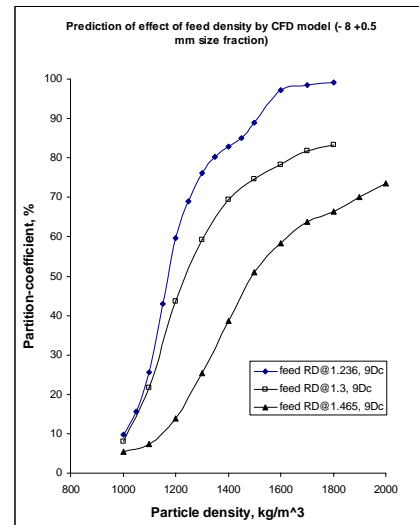

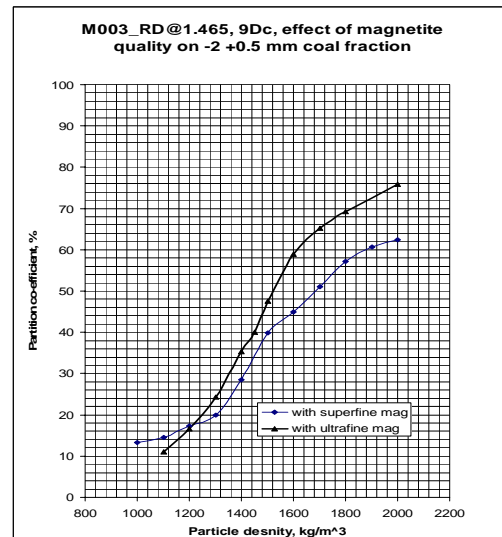Figure 9: Typical partition curves showing the effect of the relative feed medium density.

Fig 12: Comparison of fine coal (-2 +0.5 mm) partitioning curves with superfine and ultrafine mediums in DMC

To demonstrate the effect of medium size distribution on DMC performance in CFD predictions, here the two predicted partitioning curves of fine coal (-2 + 0.5 mm) are compared in Figure 12 for superfine and ultrafine magnetite mediums. As seen from Figure 12, a smaller E_p is predicted (with a consequent increase in cyclone efficiency) for ultrafine medium compared to the superfine medium, which is in consistent with the observed behaviour in dense medium cyclones [3].

Conclusions

The effect of changes in feed medium solids on dense medium cyclone performance were studied numerically using a multi-phase mixture CFD (Computational Fluid Dynamics) model for medium and air-core coupled with Lagrangian model for coal particles for a 350mm DSM cyclone. The turbulence was resolved using Large Eddy Simulation (LES). Predicted flow filed validated against LDA experimental data. The medium properties were modified by changing the particle size distribution and concentration. Three different medium sizes (ultrafine, superfine and fine) were used in the simulations.

Predicted medium segregation in side the DMC were compared with experimental data obtained by gamma ray tomography and found to be in good agreement. The effect of medium stability and rheology on DMC performance was related to feed medium size in terms of density differential and medium segregation. The simulations predicted low Ep values with ultrafine medium which gives high separation efficiency on density. A reduction in cyclone efficiency was observed for a given feed medium solids distribution at higher feed medium concentrations, due to an increase in slurry viscosity and density differential.

References

[1] Ferrara, G., State-of-the-art and New developments in dense medium separation processes, *In Proc. of Conference on Mineral processing-Recent trends and Future trends Honoring Prof.P.C.Kapoor*, IIT, Kanpur, 11-15th Dec, 1995.

[2] Klima, M.S., Killmeyer, R.P. & Hucko, R.E., Development of a Micronized-Magnetite Cycloning Process, *Proc. llth Int. Coal Prep. Congr.,* 1990, Tokyo, 145-149.

[3] He, Y.B., & Laskowski, J.S., The Effect of dense medium properties on the separation performance of a dense medium cyclone, *Minerals Engineering,* 1994, Vol. 7, Nos 2/3, pp. 209-221.

[4] Killmeyer, R.P., Maronde, C.P., Ciocco, M.V., & Zandhuis, P.H., Effects of key operational variables on mirconized-magnetite cycloning performance, *Coal Preparation,* 2002, 22, 19-40.

[5] Fourie, P.J.F., van der Walt, P.J. & Falcon, L.M., The Beneficiation of Fine Coal by Dense medium Cyclone, *J. S. Afri. Inst. Min. MetalL,* 1980, 357-361.

[6] Chedgy, D.G., Watters, L.A. & Higgins, S.T., Heavy Media Cyclone Separations at Ultra low Specific Gravity, *Prec. 10th Int. Coal Preparation Congr.,* 1986, Edmonton, Canada, vol. 1, 60-79.

[7] Stoessner, R.D.& Zawadzki, E.A., Selection of dense medium cyclone for low gravity fine coal cleaning, *In Proc. 3rd Int. Conf. on Hydrocyclones,* Oxford, England, 1987, 111-119.

[8] Collins, D.N., Napier-Munn, T.J. & Sciarone, M., The Production, Properties, and Selection of Ferrosilicon Powders for Heavy-Medium Separation, *J. S. Afri. Inst. Min. Metall.,* 1974, 103-115.

[9] Davis, J.J. & Napier-Munn, T.J., The Influence of Medium Viscosity on the Performance of Dense Medium Cyclones in Coal Preparation, *Proc. 3rd Int. Conf. on Hydrocyclones*, 1987, Oxford.

[10] Collins, D.N., Dense medium separation in cyclones, *Personal communication*, 1981.

[11] Morimoto, T.E., Laboratory Tests of the Cleaning of Fine Coal by a DSM Cyclone, *Canadian Min. Metall. Bull.*, 1952, 55, No.l, 40-48.

[12] Napier-Munn, T.J., The effecr of dense medium viscosity on separation efficiency, *Coal Preparation,* Vol.8, 1990, 145-165.

[13] Wood, J.C., A performance model for coal-washing dense medium cyclones, PhD Thesis, JKMRC, University of Queensland, 1990.

[14] Davis, J.J., A Study of Coal Washing Dense Medium Cyclones, Ph.D. Thesis, University of Queensland, 1987.

[15] Collins, B., Tumbull, T., Wright, R. & Ngan, W., Separation Efficiency in Dense Medium Cyclones, *Trans. Inst. Min. Met. Sec.C,* 1983, 92, C38-C51.

[16] Galvin, K. P., & Smitham, J. B., "Use of x-rays to determine the distribution of particles in an operating cyclone", *Minerals Engineerin*g, 1994, 7, 1269-1280.

[17] Hundertmark, A., Investigation about the solid material distribution in hydrocyclones with the aid of radioactive irradiation, *Erzmetall, BD XVIII*, 1965, H-8, 403-412.

[18] Subramanian, V.J., Measurement of medium segregation in the dense medium cyclone using gamma-ray tomography, PhD Thesis, 2002, JKMRC, University of Queensland.

[19] Suasnabar, D.J., Dense Medium Cyclone Performance, Enhancements via computational modeling of the physical process, PhD Thesis, 2002, University of New South Wales.

[20] Brennan, M.S, Subramanian, V.J., Rong, R., Holtham, P.N., Lyman, G.J., and Napier-Munn, T.J., Towards a new understanding of the cyclone separator, *Proceedings of XXII International Mineral Processing Congress*, 29 September – 3 October, 2003, Cape Town, South Africa.

[21] Narasimha M, Brennan MS, Holtham PN. Numerical simulation of magnetite segregation in a dense medium cyclone, *Minerals Engineering,* 2006; 19:1034-1047

[22] Narasimha, M., Brennan, M.S., & Holtham, P.N., CFD Modelling of Dense Medium Cyclones using Multiphase Techniques, *11th Australian Coal Preparation Conference*, Noosa Heads, Brisbane, 2007, G1, 216-228.

[23] Slack, M.D., Prasad, R.O., Bakker, A., Boysan, F., Advances in cyclone modeling using unstructured grids. *Transactions of the Institution of Chemical Engineers, Chemical Engineering Research and Design*, 2000; 78(A):1098-1104.

[24] Delgadillo, J.A., & Rajamani, R.K., A comparative study of three turbulence-closure models for the hydrocyclone problem. *Int. J. Mineral. Process,* 2005; 77(4):217-230.

[25] Brennan, M.S., CFD simulations of hydrocyclones with an air core: comparison between large eddy simulations and a second moment closure, *Chemical Engineering Research and Design.* 2006; 84A:495-505.

[26] Smagorinsky J. (1963). General circulation experiments with the primitive equations I. the basic experiment, *Monthly Weather Review,* 1963; 91:99-164.

[27] Manninen M, Taivassalo V, Kallio S. On the mixture model for multiphase flow, *Valtion Teknillinen Tutkimuskeskus,* 1996, Espoo, Finland.

[28] Saffman PG. The lift on a small sphere in a slow shear flow, *Journal of Fluid Mechanics*, 1965; 22(2):385-400.

[29] Bagnold RA. Experiments on a gravity-free dispersion of large solid spheres in a Newtonian fluid under shear, *Proceedings of the Royal Society London, Series A*, 1954; 225:49-63.

[30] Schiller L, Naumann Z., *Z. Ver. Deutsch. Ing.* 1935; 77:318.

[31] Richardson, J. R., & Zaki, W. N., Sedimentation and Fluidization: Part I, *Trans. Inst. Chem. Eng.,* 1954, 32:35-53.

[32] Mei R., An approximate expression for the shear lift force on a spherical particle at finite Reynolds number, *Int. J. Multiphase flow,* 1992; 18:145-147.

[33] Gidaspow D, Bezburuah R, Ding J. Hydrodynamics of Circulating Fluidized Beds, Kinetic Theory Approach. In Fluidization VII, *Proceedings of the 7th Engineering Foundation Conference on Fluidization,* 1992, pages 75-82.

[34] Ishii M, Mishima K. Two-fluid model and hydrodynamic constitutive relations, *Nuclear Engineering and design*, 1984; 82:107-126.

[35] Hirt CW, Nichols BD. Volume of fluid (VOF) method for the dynamics of free boundaries, *Journal of Computational Physics*, 1981; 39:201-225.

[36] Fanglu, G., & wenzhen, L., Measurement and Study of Velocity Field in Various Cyclones by Use of Laser Doppler Anemometry, *In Proc. of. 3rd International Conference on Hydrocylones*, Oxford, England, 30 September, 1987.